buildings

MDPI

Article

Digital Twin Evaluation of Environment and Health of Public Toilet Ventilation Design Based on Building Information Modeling

Liang Zhao [1], Hong Zhang [1,2,*], Qian Wang [3,*], Bo Sun [1], Wenhui Liu [1], Kaichen Qu [1] and Xiumei Shen [1]

[1] School of Architecture, Southeast University, Nanjing 210096, China; zhaoliang2019@seu.edu.cn (L.Z.); 230218016@seu.edu.cn (B.S.); 230179002@seu.edu.cn (W.L.); 230208472@seu.edu.cn (K.Q.); 230198008@seu.edu.cn (X.S.)
[2] Key Laboratory of Urban and Architectural Heritage Conservation, Ministry of Education, Southeast University, Nanjing 210096, China
[3] Department of Building, School of Design and Environment, National University of Singapore, Singapore 117566, Singapore
* Correspondence: zhangseu@aliyun.com (H.Z.); bdgwang@nus.edu.sg (Q.W.)

Abstract: Poor indoor air quality reduces the comfort experienced in the environment and can also harm our physical health. Mechanical ventilation design plays an important role in improving the indoor environment and the safety of public toilets. Therefore, in this study, we aimed to evaluate public toilet ventilation design schemes through a digital twin to determine the most effective scheme for reducing indoor pollutant concentrations. In this study, we used Autodesk Revit to create a digital twin BIM of different ventilation systems. We simulated the diffusion of pollutants in these models using computational fluid dynamics (CFD)-based methods, and we used DesignBuilder to simulate building energy consumption. From the perspective of architectural design, we determined measures important for reducing the concentration of air pollutants by increasing the number and volume of air exchanges and controlling the installation height of exhaust vents. The results show that the ventilation design of an all-air air conditioning system with an exhaust height of 400 mm can remarkably improve the indoor environmental health and ventilation efficiency of public toilets, while consuming 20.4% less energy and reducing carbon emissions by 30,681 kg CO_2.

Keywords: public toilets; ventilation; digital twin; concentration of indoor pollutants; computational fluid dynamics (CFD)

Citation: Zhao, L.; Zhang, H.; Wang, Q.; Sun, B.; Liu, W.; Qu, K.; Shen, X. Digital Twin Evaluation of Environment and Health of Public Toilet Ventilation Design Based on Building Information Modeling. *Buildings* **2022**, *12*, 470. https://doi.org/10.3390/buildings12040470

Received: 4 March 2022
Accepted: 7 April 2022
Published: 11 April 2022

1. Introduction

Indoor air quality (IAQ) is closely related to human lives. Poor indoor air quality not only reduces environmental comfort but can also harm our health [1]. As an indoor space with a unique service type, the air environment in toilets is often neglected due to the short time people spend there [2,3]. Therefore, maintaining high environmental quality in toilets is a matter of concern. Since the frequency of use and the time people occupy public toilets are much higher than those of residential toilets, guaranteeing the air quality of public toilets is more challenging [4]. According to the hygienic standard for communal toilets in cities, the main pollutants in public toilets are ammonia (NH_3) and hydrogen sulfide (H_2S) [5]. Ammonia and hydrogen sulfide can easily irritate people's skin, respiratory tract, and eyes, and may cause headache, dizziness, blurred consciousness, and even coma in severe cases [6]. In the process of designing the ventilation of public toilets, selecting an appropriate ventilation system that can effectively improve the IAQ and avoid the harmful gas emissions that adversely affect the surrounding environment is key [7,8]. Therefore, in this study, we simulated different air distributions during the design phase of public toilets to find a ventilation method that can effectively reduce the air pollutant concentration inside public toilets.

Numerical simulations based on computational fluid dynamics (CFD) are widely used in the field of building ventilation design. CFD can be used to more accurately simulate indoor airflow organization, pollutant propagation paths, and other phenomena to reduce both the costs and risks during the design phase [9]. Gu et al. [10] used CFD to simulate the influence of harmful gases in the toilets of temporary hospitals on the indoor environment of the building, and further analyzed and evaluated the influence of different ventilation system design schemes on the diffusion of harmful gases. Zhang et al. [4] showed that standard k-ε, RNG k-ε, realizable k-ε, and low-Re k-ε models consider the natural buoyancy-driven convection during the diffusion process and can be used to simulate indoor pollutant diffusion. Lee et al. [9] performed a steady-state analysis of temperature and flow velocity inside the building using the turbulence model of the standard k-e model. Therefore, this study will use the standard k-ε model to simulate indoor pollutant dispersion.

Wan and Chao [11] studied the importance of ventilation systems on pollutant diffusion and found that one-way upper and one-way lower ventilation systems are more effective in reducing the influence of aerosol distribution. The ASHRAE study showed that heating, ventilation, and air conditioning (HVAC) systems can effectively reduce the concentration of viruses and harmful gases in the air, thus reducing the risk of virus and harmful gas transmission [12]. However, few researchers and designers have studied the effective ventilation system design and the factors influencing building space ventilation in order to reduce the impact of harmful gases and indoor pollutants [13,14]. Given the effects of the IAQ in public toilets on human health, studying the distribution law of pollutant concentration in public toilets is important. Digital twin models of public toilets have been constructed to simulate different indoor ventilation systems, providing guidance for reasonably designing the ventilation of public toilets [15,16]. These models are essential for improving hygiene in public toilets and for reducing the risk of infection.

A digital twin refers to the construction of models in digital virtual space to enable the analysis and optimization of entities in physical space [17]. In the architectural design phase, digital twin technology can be used to improve the accuracy of ventilation design and to verify the real-world performance of the design scheme [18]. Building Information Modeling (BIM) is a data-, information-, and knowledge-sharing center; in the architectural design process, BIM can provide rich information. As a digital technology in the construction industry, BIM is used to simulate building information through numerical simulation in the design phase. Zhao et al. [19] integrated BIM models with DesignBuilder to evaluate the feasibility of nearly zero-energy building retrofit schemes for existing buildings. Delavar et al. [20] proposed a digital twin evaluation framework in the architectural design phase and found that the BIM and CFD models of the level of development (LOD) 300 can be effectively integrated. Therefore, in this study, we used the BIM LOD300 model coupled with CFD software to simulate the performance of different ventilation design schemes, and DesignBuilder to simulate building energy consumption and the indoor comfort of the design scheme.

The ventilation design of public toilets mainly considers the use of negative pressure to discharge the foul smells generated by the toilet. Under natural ventilation conditions, ensuring that the public toilet is in a negative pressure state relative to other public areas is difficult, and the air in the surrounding public areas can be easily polluted [21]. Therefore, the standard for the design of civil buildings requires the installation of a mechanical exhaust system to ensure the air quality in public toilets and the surrounding areas [22]. At present, a clear value in the relevant specifications for the selection of the frequency of air exchanges in public toilets is not provided, and most of the values are derived from engineering practice experience. This has led to the waste of energy due to excessive ventilation in the public toilets, and the pollutants in the toilets cannot be effectively discharged with insufficient ventilation [22,23]. Different design codes describe various requirements regarding the frequency of air exchanges in the toilet (Table 1). Although the relevant specifications stipulate the corresponding values for the frequency of air exchanges

and the ventilation volume in the toilet, they do not describe the form of the exhaust system, the frequency of air exchanges, or the installation height of the exhaust vents [6,22,24]. Therefore, in this study, we adopted a numerical simulation to analyze the influence of different ventilation system design schemes of public toilets on the IAQ.

Table 1. Recommended ventilation parameters for public toilets.

Number	Technical Standard	Frequency of Air Exchanges (h^{-1})
1	Standard for design of urban public toilets (CJJ14-2016)	≥5 and ≥(Db × 40 + Xb × 20)/V
2	Design code for heating ventilation and air conditioning of civil buildings (GB50736-2012)	5–l5
3	National Technical Measures for Design of Civil Construction Heating, Ventilation and Air Conditioning	10–20

Note: Db, stool; Xb, urinal; V, ventilated space volume.

The design of public toilet ventilation systems plays a crucial role in improving indoor air quality and reducing the diffusion of pollutants [7,13]. In the public toilet design stage, various air supply, and exhaust schemes are simulated, and the most reasonable airflow organization and ventilation strategy to prevent the spread of pollutants are selected. CFD is used to simulate the ventilation performance of different HVAC systems [23,25,26]. To verify numerical simulations, grid-line-independent verification of the digital twin model is performed. Then, the validated numerical method is used to analyze the effects of different ventilation systems (with different numbers of air exchanges, ventilation modes, and exhaust vent heights) on the IAQ. Quantitative analysis and evaluation of the average concentration of indoor pollutants (ACIPs), ventilation efficiency, and the age of air (AOA) in ventilation design schemes are conducted. DesignBuilder is used to simulate public toilet energy consumption. Finally, different ventilation design schemes are evaluated through a digital twin, and a ventilation design scheme that reduces the ACIPs is constructed. The ventilation design scheme of the ideal HVAC system in the public toilet is explored.

2. Materials and Methods

This study mainly studied the influence of different ventilation design schemes on the distribution of pollutants in public toilets. We established corresponding digital twin models for different ventilation systems designed, and supplemented the design of ventilation systems by quantitative assessment of the diffusion of harmful gases to effectively improve the indoor air quality in public toilets. Figure 1 shows the framework of our digital twin evaluation method for public toilets.

BIM can be regarded as a collaborative tool used in different disciplines in the architectural design phase (Figure 1). BIM provides shared geometric data for CFD, the building energy model (BEM), and indoor comfort simulations, and attribute information provides the boundary conditions, such as velocity, temperature, and concentration required for the simulation. In this study, we used the Revit of Autodesk to create a BIM, and Revit software provided the interface for collaborative software data transfer. We divided thermal zones in Revit and exported the gbXml data to Design Builder to simulate building energy consumption. We exported SAT-format data to ICEM CFD for meshing and part division. Finally, we used the Ansys Fluent commercial software to numerically simulate the airflow distribution in public toilets. We mainly focused on the numerical simulation and energy consumption simulation analysis of the air environment in public toilets, and selected a suitable ventilation design system based on the evaluation index.

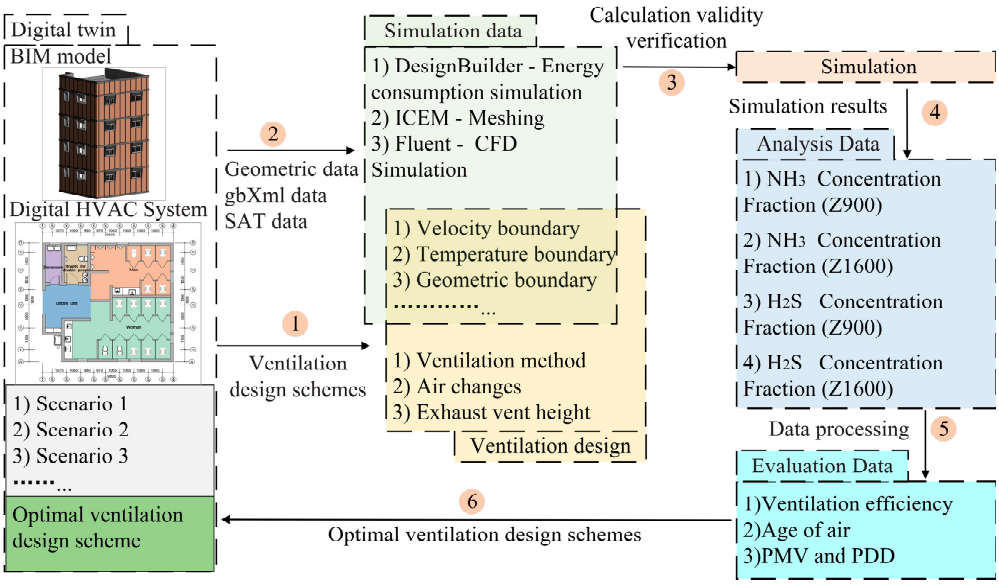

Figure 1. Digital twin evaluation method framework.

2.1. Evaluation Method

The criteria used to evaluate the IAQ mainly include the pollutant concentration in the personal breathing zone, ventilation rate, the AOA, building energy consumption, and the thermal comfort index. The indices used to evaluate indoor thermal comfort mainly include the predicted mean vote (*PMV*) and the predicted percentage of dissatisfied (*PPD*) to express the percentage of those satisfied and dissatisfied with the indoor environment, respectively.

2.1.1. Pollutant Concentration

The concentration of pollutants in a personal breathing zone directly reflects whether human health requirements are met. As people squat and stand when they go to the toilet, we selected the vertical heights of 0.9 m (Z900) and 1.6 m (Z1600) from the ground as the height of the breathing zone [1,16]. We used the maximum concentration of pollutants specified in the Hygienic Standard for Communal Toilets in Cities as the reference limit for concentrations of NH_3 ($\leq$0.30 mg/m^3) and H_2S ($\leq$0.01 mg/m^3) in public toilets [5]. Therefore, as pollutants, we considered the harmful gases NH_3 and H_2S from toilets in this study.

2.1.2. Pollutant Concentration

Ventilation efficiency is an indicator that expresses the ability of ventilation to remove pollutants, and is commonly referred to as sewage efficiency [27]. For the same pollutant, the airflow that can maintain a lower indoor pollutant concentration or can quickly reduce the initial concentration of indoor pollutants with the same air supply volume has a high pollutant discharge efficiency. The ventilation efficiency is expressed as:

$$E_C = \frac{C_e - C_{in}}{C - C_{in}} \quad (1)$$

where E_c is the ventilation efficiency, C_e is the concentration of pollutants in an exhaust vent, C_{in} is the concentration of pollutants in the air supply vent, and C represents the average concentration of pollutants in indoor personal breathing zones.

2.1.3. Age of Air

Air age refers to the time elapsed from the time the air particles enter the room to a certain point in the room, reflecting the freshness of the indoor air. Air age can be used to

comprehensively measure the ventilation effect in a room and is an important indicator for evaluating the IAQ [28]. In general, the younger the age of the air, the higher the IAQ.

2.1.4. PMV and PPD

PMV is an index used to evaluate the thermal response of the human body (the feeling of heat and cold) and represents the average feeling of cold and heat of most people in the same environment. When *PMV* = 0, the indoor thermal environment is in the best thermal comfort state [29–31]. The design code for heating ventilation and air conditioning of civil buildings stipulates that the thermal comfort in heating and air-conditioned rooms should be evaluated using *PMV* and *PPD* in accordance with moderate thermal environments. *PMV* and *PDD* indices must be determined to ensure the specifications of the conditions for thermal comfort are met. Acceptable values are: $-1 \leq PMV \leq +1$ and $PPD \leq 27\%$ [32].

$$PMV = [0.303 \times \exp(-0.036 \times M) + 0.0275] \times TL \quad (2)$$

where M is the energy metabolism rate of the human body, which is determined by the amount of activity of the human body (unit: W/m^2); TL is the difference between the amount of heat produced by the human body and the amount of heat the body emits to the outside world. Table 2 show the thermal sensation scale of the *PMV*.

Table 2. Thermal sensation scale of the *PMV*.

PMV	**−3**	**−2**	**−1**	**0**	**1**	**2**	**3**
Thermal sensation	cold	cool	slightly cool	neutral	slightly warm	warm	hot

The *PPD* is the average vote of the population that is dissatisfied with their thermal environment. The *PPD* index predicts the feeling of being too warm or too cold in a population [32]:

$$PPD = 100 - 95 \times \exp[(0.03353 \times PMV^4 + 0.21 \times PMV^2)] \quad (3)$$

where *PMV* is the evaluation index that characterizes the human body's thermal response (feeling of heat and cold).

2.2. Digital Twin Models

We conducted our study case in Nanjing, China. The toilet consisted of four floors, each with an area of 92.7 m^2. The architectural design plan and BIM of this study case are shown in Figure 2. According to the architectural design scheme, we established the public toilet to determine the air supply and exhaust design plan (as shown in Figure 2) and created the corresponding BIM. To not affect the calculation, we reasonably simplified the shape of the urinals and toilets. We took the room length as the x-axis (9800 mm), the room width as the y-axis (9600 mm), and the room height as the z-axis (3000 mm, with a ceiling height of 2600 mm). The public toilet contained 5 urinals and 14 toilets. The size of the urinal was 350 × 350 × 600 mm^3, and the urinals were 600 mm from the ground. Each urinal was evenly spaced 800 m apart, and the corresponding hole diameter of the urinal was 70 mm. The size of the toilet was 350 × 350 × 100 mm^3, with partitions around each toilet to form a semi-closed toilet seat. The length of a single toilet seat was 1500 mm and the width was 1000 mm, the height of the partition was 1900 mm (150 mm from the ground), and the diameter of the corresponding opening of the toilet was 110 mm. The size of the door opening was 2000 × 2200 mm^2.

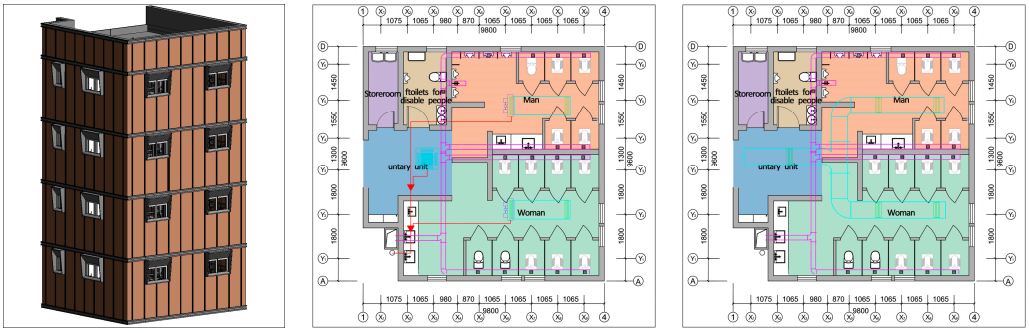

(**a**) (**b**) (**c**)

Figure 2. Three-dimensional view and layout of a typical floor of the public toilet facility. (**a**) Description of three-dimensional view; (**b**) Description of primary air fan–coil system; (**c**) Description of all-air air conditioning system.

To study the influence of the air supplied in the public toilet ventilation system and the layout of the exhaust vents on the diffusion of harmful gases, we considered two different ventilation systems in the analysis (Figure 2). These two ventilation systems were the primary air fan–coil system and the all-air air conditioning system, which have different airflow organizations. To ensure the negative pressure in public toilets, the air supply volume of all-air air conditioning systems must be 80% of the exhaust air volume, and the remaining air volume is supplemented by door opening [22].

The building layout and ventilation system were independent of each other, and the ventilation design followed the building layout. We designed different ventilation design schemes and designed them according to the frequency of air exchanges, the ventilation method, and the height of the exhaust vent. The main aspects of this study included: (1) examining the distribution of pollutants in public toilets for different ventilation times by changing the frequency of air exchanges, the ventilation method, and the height of the exhaust vent; (2) according to the frequency of air exchanges, differing the air-conditioning system and the height of the exhaust vent to analyze the change in energy consumption in each scenario; (3) analyzing the concentrations of indoor pollutants, the AOA, ventilation efficiency, and *PMV-PPD* evaluation indicators in different scenarios, and recommending suitable ventilation schemes.

2.3. Digital Twin Models

CFD technology can be used to quantitatively analyze the diffusion trajectory of harmful gases and the concentration distribution of harmful gases in space, which can provide a reference for public toilet ventilation design. In this study, we established a CFD calculation model for the design process of public toilets, and simulated the air flow using the standard k-ε turbulence model.

2.3.1. Boundaries

Because ammonia and hydrogen sulfide are harmful, in-person experiments are not advisable. These dangerous experiments can be effectively replaced by the combination of a BIM and digital twin evaluation and the use of numerical simulation experiments. Table 3 shows the boundary conditions for door openings, walls, and major pollutants in this study. Table 4 shows the boundary conditions of the primary air fan–coil system.

Table 3. Door openings, walls, and pollutant boundary conditions.

Number	Boundary	Description	
1	door openings	Set the door opening as a free outflow boundary, the temperature in winter is 20 °C, and the design temperature in summer is 26 °C [22].	
2	walls	Set the walls and partitions around the room as wall boundary conditions, and the heat transfer coefficient is 0.6 W/ (m^2 K) [22].	
3	pollutants	NH_3	NH_3 release rate from the urinal is 0.065 m/s, 0.00005 kg/m^3 [1,4].
			NH_3 release rate from the toilet is 0.05 m/s at 0.00005 kg/m^3 [1,4].
		H_2S	H_2S release rate of the toilet is 0.03 m/s, 0.00002 kg/m^3 [1,4].

Table 4. Mechanical exhaust and door opening boundary conditions.

	Multi-Connected Indoor Unit			
	Air supply		Return air	
	Velocity (m/s)	Tuyere area (m^2)	Velocity (m/s)	Tuyere size (mm)
Primary air fan–coil system	3.148	0.0353	2.778	400 × 400
	Fan coil			
	Air supply		Return air	
	Velocity (m/s)	Tuyere size(mm)	Velocity (m/s)	Tuyere size(mm)
	3.08	120 × 750	3.08	120 × 750

2.3.2. Calculation Model Validation

Using a suitable number of grids ensures a small calculation error, so that accurate simulation results can be obtained. A structured grid can better ensure the quality and quantity of the grid. Therefore, in this study, we used a tetrahedral-structured grid to divide the model of the public building, and the air supply vents, exhaust vents, pollution sources, and door openings were properly locally encrypted. We used CFD to divide the space that required a numerical model into a finite number of meshes to calculate fluid flow, so an appropriate mesh design is crucial for the calculation results. To ensure the accuracy and feasibility of the numerical simulation, the mesh of the model needs to be properly optimized. In this study, the computer of Lenovo P50 was used as the computing resource. The grid independence verification of the primary air fan–coil system with 15 air exchanges is shown in Table 5.

Table 5. Mesh sensitivity.

Meshing	Number of Cells	Frequency of Air Exchanges (h^{-1})	Height (mm)	Maximum Velocity		Averaged Velocity	
				Velocity (m/s)	Relative Error (%)	Velocity (m/s)	Relative Error (%)
Coarse	2,975,007	15	900	0.44	22.73	0.42	21.43
			1600	0.45	15.56	0.44	20.45
Middle	4,286,976		900	0.34	8.82	0.33	9.09
			1600	0.38	−2.63	0.35	−5.71
Fine	9,313,280		900	0.31	−3.23	0.3	−3.33
			1600	0.39	0	0.37	2.70
Finest	11,439,669		900	0.32	/	0.31	/
			1600	0.39	/	0.36	/

To determine the appropriate number of computing grids, we conducted corresponding simulation calculations for four different grid numbers: 2,975,007, 4,286,976, 9,313,280, and 11,439,669 (shown in Table 5). The same simulation conditions were set for the four mesh numbers and each was iterated until the simulation converged. Comparing the maximum and average velocities of points in the toilet, the results showed that 9,313,280 grids were sufficient to achieve grid independence, and the relative error between the maximum and average velocities was less than 5%. The average speed complied with the requirement of the design code for heating ventilation and air conditioning of civil buildings of less than 0.5 m/s.

3. Results

Public toilets are places where people gather, and indoor pollutants are difficult to control if ventilation is poor. We used CFD technology to simulate the air flow of different ventilation systems to verify the accuracy of the computational model simulation. On this basis, we analyzed the influence of different numbers of air exchanges, different air conditioning systems, and different exhaust vent heights on the diffusion of indoor air pollutants to determine the optimal ventilation method and the most appropriate exhaust vent installation positions.

3.1. Effect of the Frequency of Air Exchanges

Good airflow organization is the main measure used to control the diffusion of pollutants through ventilation, and the specific frequency of air exchanges is difficult to determine. Table 6 shows the boundary conditions for the different numbers of air exchanges that we used to study their effect on the ACIPs.

Table 6. Boundary conditions for the frequency of air exchanges.

Scenario	Ventilation System	Exhaust Vent Height (mm)	Frequency of Air Exchanges (h^{-1})	Exhaust Volume (m^3/h)	Exhaust Vent Velocity (m/s)
1	primary air fan-coil system	2600	5	1390.5	2.10
2			10	2781	2.10
3			15	4171.5	2.10
4			20	5562	2.10

Figure 3 shows the concentration cloud map of indoor pollutants for Scenario 1. The average concentrations of H_2S are 0.0229 (Z900) and 0.0225 mg/m^3 (Z1600). The average concentrations of NH_3 are 0.76 (Z900) and 0.6755 mg/m^3 (Z1600).

Figure 4 shows the concentration cloud map of indoor pollutants for Scenario 2. The average concentrations of H_2S are 0.0126 (Z900) and 0.0124 mg/m^3 (Z1600). The average concentrations of NH_3 are 0.298 (Z900) and 0.2933 mg/m^3 (Z1600).

Figure 5 shows the concentration cloud map of indoor pollutants for Scenario 3. The average concentrations of H_2S are 0.0079 (Z900) and 0.0078 mg/m^3 (Z1600). The average concentrations of NH_3 are 0.2032 (Z900) and 0.1971 mg/m^3 (Z1600).

Figure 6 shows the concentration cloud map of indoor pollutants for Scenario 4. The average concentrations of H_2S are 0.0063 (Z900) and 0.0062 mg/m^3 (Z1600). The average concentrations of NH_3 are 0.1583 (Z900) and 0.1549 mg/m^3 (Z1600).

With the increase in the frequency of air exchanges, the overall pollutant concentration in the toilet substantially improves, the urinal room has better air mobility because there is no partition, and the exhaust effect is much stronger than that of the toilet room. When the frequency of air exchanges increases to 15 h^{-1} (Scenario 3), both H_2S and NH_3 meet the requirements of the Hygienic Standard for Communal Toilets in Cities, but part of the partition does not meet the requirements.

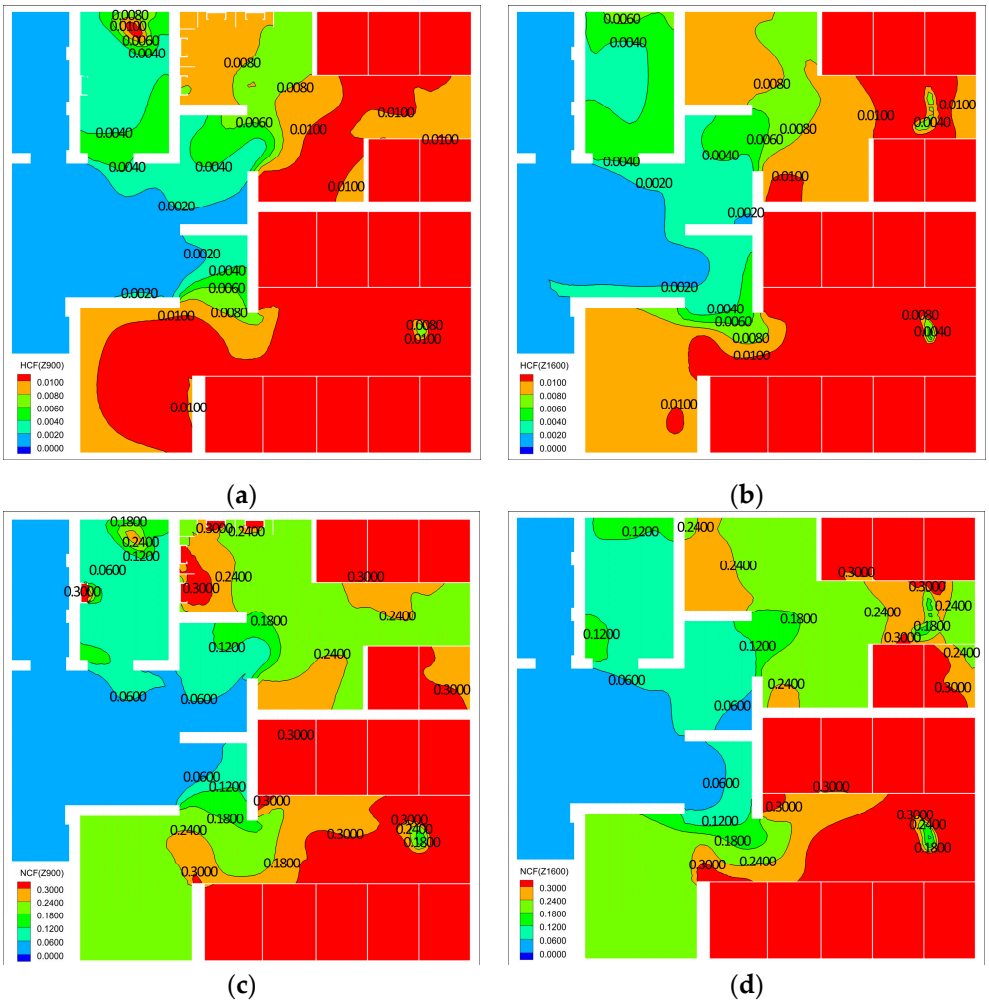

Figure 3. Concentration cloud map of pollutants in Scenario 1. (**a**) H_2S concentration fraction (Z900); (**b**) H_2S concentration fraction (Z1600); (**c**) NH_3 concentration fraction (Z900); (**d**) NH_3 concentration fraction (Z1600).

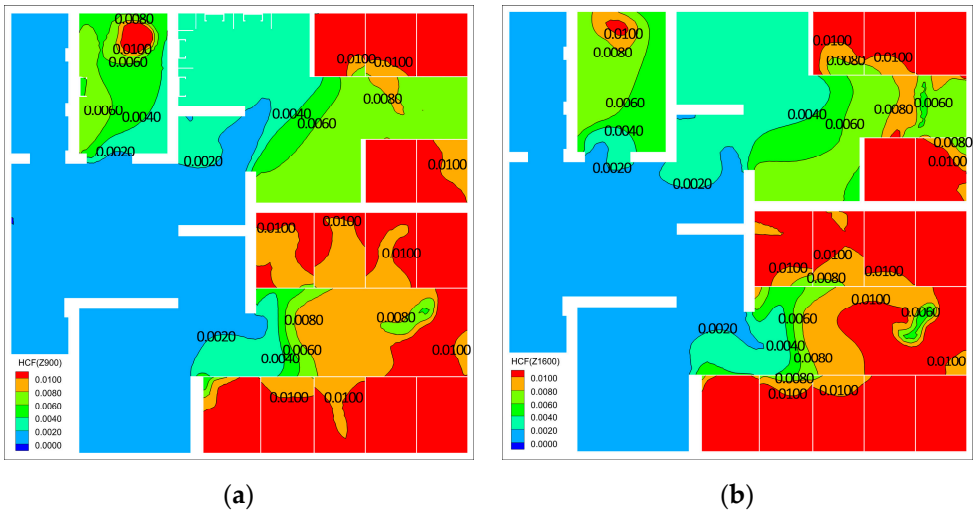

Figure 4. *Cont.*

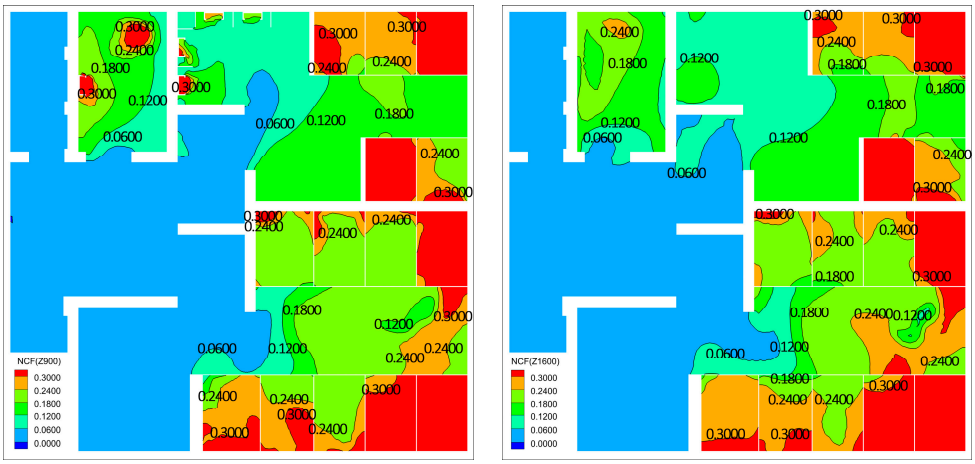

Figure 4. Concentration cloud map of pollutants in Scenario 2. (**a**) H_2S concentration fraction (Z900); (**b**) H_2S concentration fraction (Z1600); (**c**) NH_3 concentration fraction (Z900); (**d**) NH_3 concentration fraction (Z1600).

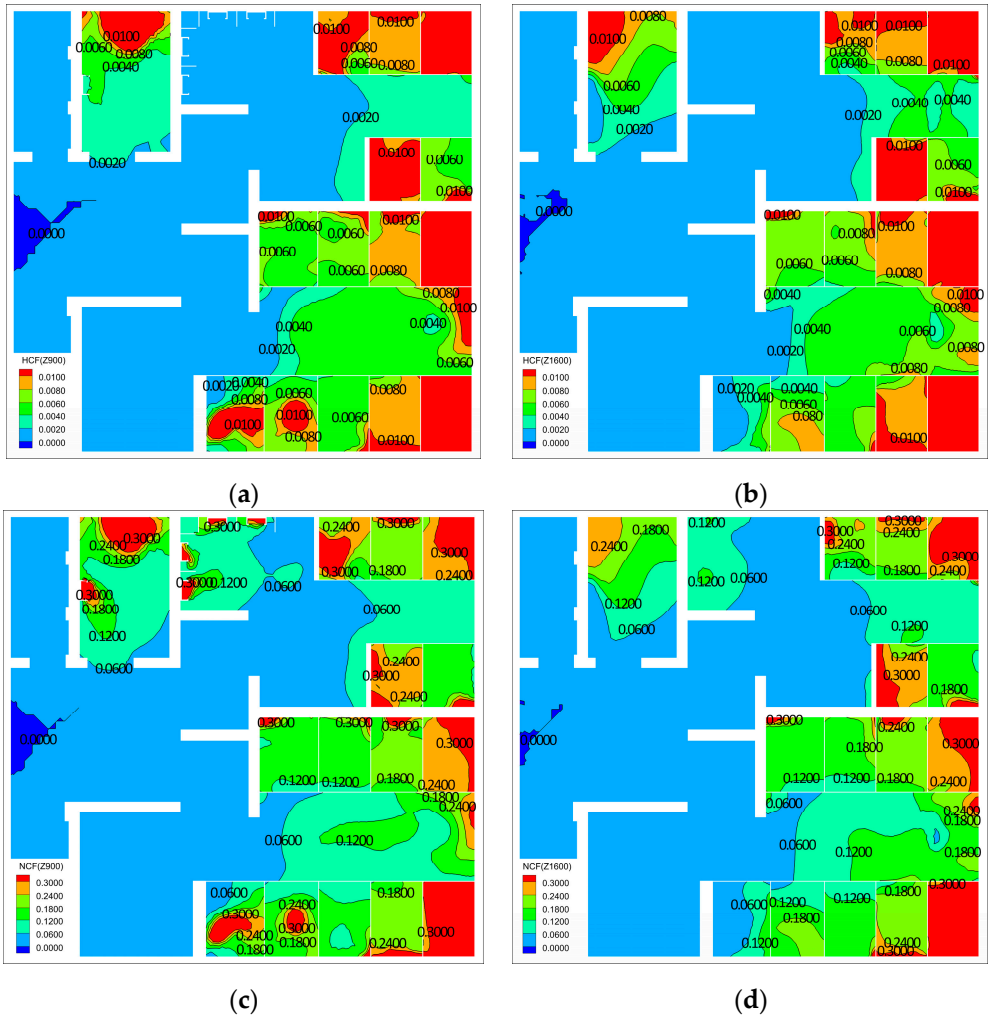

Figure 5. Concentration cloud map of pollutants in Scenario 3. (**a**) H_2S concentration fraction (Z900); (**b**) H_2S concentration fraction (Z1600); (**c**) NH_3 concentration fraction (Z900); (**d**) NH_3 concentration fraction (Z1600).

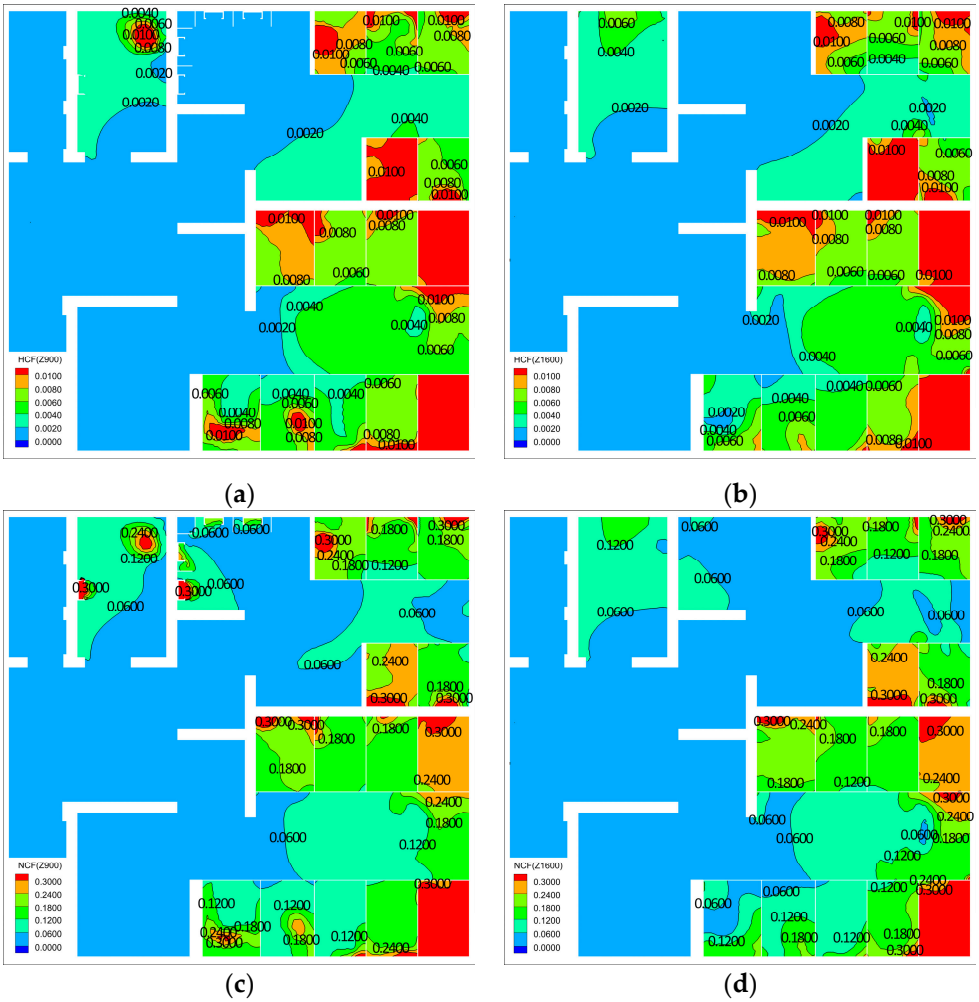

Figure 6. Concentration cloud map of pollutants in Scenario 4. (**a**) H_2S concentration fraction (Z900); (**b**) H_2S concentration fraction (Z1600); (**c**) NH_3 concentration fraction (Z900); (**d**) NH_3 concentration fraction (Z1600).

Figure 7 shows the variation trend in the average ACIPs with the frequency of air exchanges. As the frequency of air exchanges increases, the ACIPs gradually decrease, but the downward trend gradually slows. With the increase in the frequency of air exchanges, the difference between the concentrations of Z900 and Z1600 pollutants gradually decreases. The ACIPs do not decrease obviously when the frequency of air exchanges increases from 15 to 20 h^{-1}; especially, the pollution concentration in the partition tends to be stable. Therefore, from the perspective of energy savings and emission reduction, in the following, we adopted 15 h^{-1} as the frequency of air exchanges.

3.2. Effect of Exhaust Vent Velocity

The air velocity of the exhaust vent is an important factor controlling the ACIPs. If the air velocity of the exhaust vent is too low, indoor pollutants cannot be effectively removed. If the air velocity of the exhaust vent is too high, indoor air disturbances increase, resulting in air stagnation. Table 6 shows the boundary conditions of the air velocity of the exhaust vent used to simulate the effect of the exhaust vent velocity on the diffusion of indoor pollutants. According to the National Technical Measures for Design of Civil Construction: Heating, Ventilation and Air Conditioning, the wind speed of the exhaust vents in public toilets should be 1–5 m/s, so we used this wind speed for the exhaust vents in this study, as shown in Tables 6 and 7.

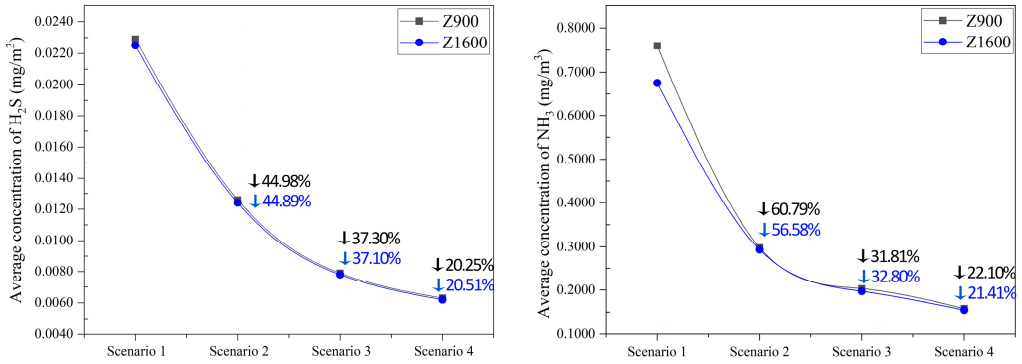

(**a**) (**b**)

Figure 7. Variation trend in the ACIPs with the frequency of air exchanges. (**a**) Average concentration of H_2S; (**b**) Average concentration of NH_3.

Table 7. Boundary conditions for air velocity at exhaust vent.

Scenario	Ventilation System	Exhaust Vent Height (mm)	Frequency of Air Exchanges (h^{-1})	Exhaust Volume (m^3/h)	Exhaust Vent Velocity (m/s)
5	primary air fan-coil system	2600	15	4171.5	4.03
6					3.03
7					1.10

According to the simulation results of Scenarios 3, 5, 6 and Scenario 7, the ACIPs in the public toilet vary with the velocity of the exhaust vent, as shown in Figure 8. Since NH_3 is less dense than air and H_2S is denser than air, when the velocity of the exhaust vent is lower, the power of mechanical exhaust is also weaker. At this time, rising buoyancy plays a leading role in the diffusion of pollutants. With the increase in the velocity of the exhaust vent, the indoor air disturbance increases and the pollutants are not easily discharged outdoors.

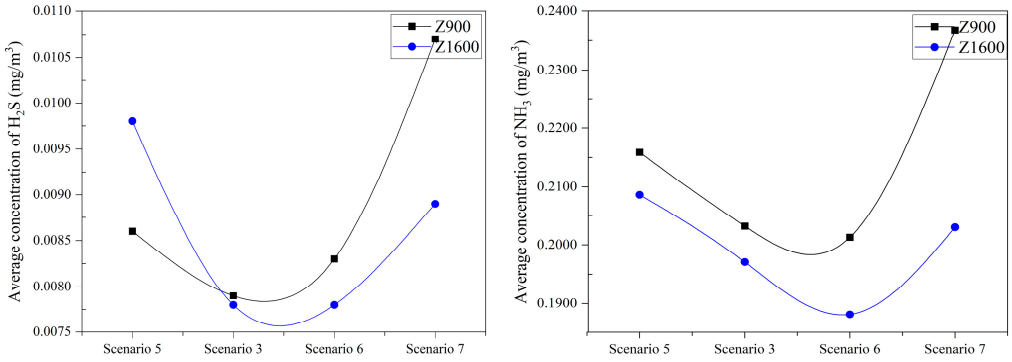

(**a**) (**b**)

Figure 8. Variation trend in the ACIPs with different exhaust vent air velocities. (**a**) Average concentration of H_2S; (**b**) Average concentration of NH_3.

Compared to Scenario 3, the H_2S concentration in Scenario 6 decreased by -1.22% (Z900) and 0% (Z1600), and the NH_3 concentration decreased by 6.76% (Z900) and 9.86% (Z1600). Although the average H_2S concentration in Scenario 3 is higher than that in Scenario 6, the decrease in the average concentration of NH_3 in Scenario 3 is larger than the increase in H_2S in Scenario 6. Therefore, in subsequent studies, we adopted an exhaust vent velocity of 3.03 m/s in Scenario 6.

3.3. Effect of Air Conditioning System

According to the all-air air conditioning system shown in Figure 2, the boundary conditions of the all-air air conditioning system are shown in Table 8. The frequency of air exchanges was 15 h^{-1} and the velocity of the exhaust vent was 3.03 m/s to study the influence of different air conditioning systems on indoor pollutants.

Table 8. The all-air air conditioning system boundaries.

Scenario	Ventilation System	Exhaust Vent Height (mm)	Frequency of Air Exchanges (h^{-1})	Exhaust Volume (m^3/h)	Supply-Air Velocity (m/s)
8	All-air air conditioning system	2600	15	4171.5	3.13

Figure 9 shows the concentration cloud map of indoor pollutants for Scenario 8. The average H_2S concentrations are 0.0078 (Z900) and 0.0068 mg/m^3 (Z1600). The average concentrations of NH_3 are 0.1810 (Z900) and 0.1515 mg/m^3 (Z1600).

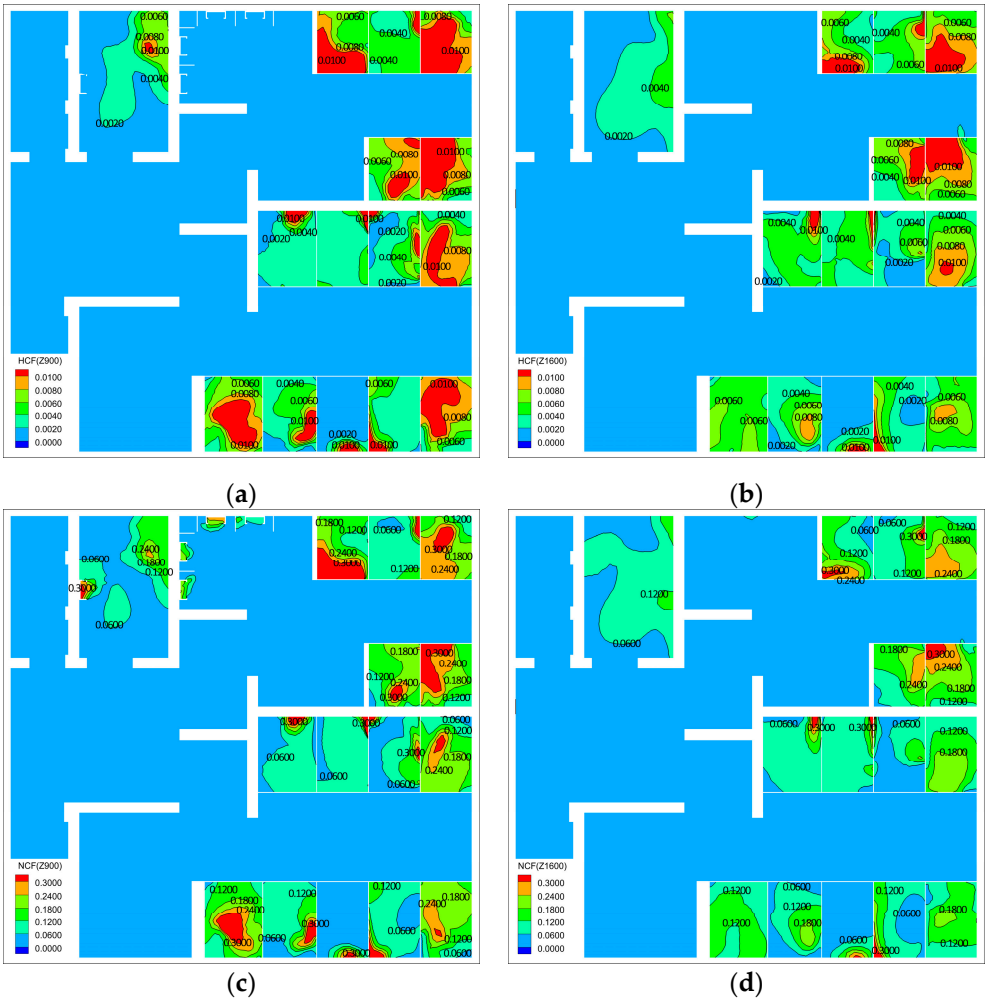

Figure 9. Concentration cloud map of pollutants in Scenario 8. (**a**) H_2S concentration fraction (Z900); (**b**) H_2S concentration fraction (Z1600); (**c**) NH_3 concentration fraction (Z900); (**d**) NH_3 concentration fraction (Z1600).

The air supply speed in Scenario 8 is 3.13 m/s, which is close to the air supply velocity in Scenario 6. However, in Scenario 8, the air supply from the door opening only accounts for 20% of the total air supply and the rest is sent into the room through the indoor air vent.

Compared to Scenario 3, the distribution of air supply vents in Scenario 8 is more dispersed and the ACIPs are lower.

The numerical simulation results for Scenarios 6 and 8 are shown in Table 9. The calculation results showed that the all-air air conditioning system can reduce the ACIPs by more than 5%. Therefore, we used the all-air air conditioning system to study the distribution of indoor pollutants.

Table 9. The ACIPs with an all-air air-conditioning system in different scenarios.

ACIPs		Scenario 6	Scenario 8	Reduction (%)
H_2S (mg/m^3)	Z900	0.0083	0.0078	5.77
	Z1600	0.0078	0.0068	13.18
NH_3 (mg/m^3)	Z900	0.2013	0.1810	10.08
	Z1600	0.1881	0.1515	19.46

3.4. Effect of Supply-Air Velocity

The Section 3.3 calculation results showed that the all-air air conditioning system has advantages over the primary air fan–coil system in reducing the ACIPs. The boundary conditions of the all-air air conditioning system are shown in Table 10 to demonstrate the influence of different supply-air velocities of the all-air air conditioning system on the distribution of indoor pollutants.

Table 10. Boundary conditions of supply-air velocity.

Scenario	Ventilation System	Exhaust Vent Height (mm)	Frequency of air Exchanges (h^{-1})	Exhaust Volume (m^3/h)	Supply-Air Velocity (m/s)
9	all-air air conditioning system	2600	15	4171.5	1.05
10					2.02
11					4.12

Figure 10 shows the variation in the ACIPs in a public toilet facility with an all-air air conditioning system with different air supply vent velocities. With the increase in supply-air velocity, the average concentration of indoor NH_3 showed a downward trend, but the downward trend gradually decreased. The average concentration of H_2S first decreased and then increased with the increase in supply-air velocity. The average concentrations of indoor pollutants in Scenarios 8, 10, and 11 are basically the same. Therefore, to minimize the average concentration of NH_3, we selected 3.13 m/s as the supply-air velocity.

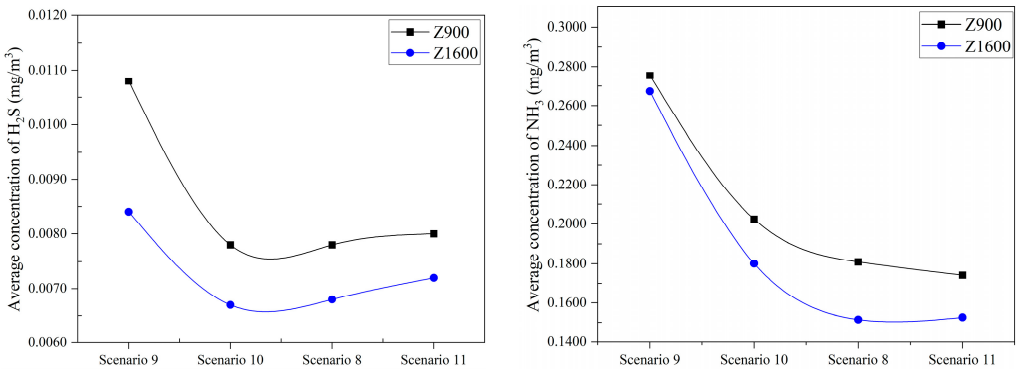

(**a**) (**b**)

Figure 10. Variation trend in the ACIPs with supply-air vent velocities. (**a**) Average concentration of H_2S; (**b**) Average concentration of NH_3.

3.5. Effect of the Height of the Exhaust Outlet

Scenario 8 has a clear advantage over the other scenarios with the all-air air conditioning system. Table 11 shows the boundary conditions of the height of the exhaust vent of the all-air air conditioning system that we used to study the effect of different exhaust vent heights on indoor pollutant concentrations.

Table 11. Boundary conditions for exhaust vent height.

Scenario	System	Exhaust Vent Height (mm)	Frequency of Air Exchanges (h^{-1})	Supply-Air Velocity (m/s)	Air-Outlet Velocity (m/s)
12	all-air air conditioning system	100	15	3.13	3.03
13		400			
14		700			
15		1000			
16		1300			
17		1600			

According to the calculation results using the boundary conditions listed in Table 11, as shown in Figure 11, we found that the ACIPs gradually increases with the increase in the height of the exhaust vent. Therefore, the closer the exhaust vent to pollutants, the more indoor pollutants are removed. Therefore, the side exhaust has advantages over the top exhaust.

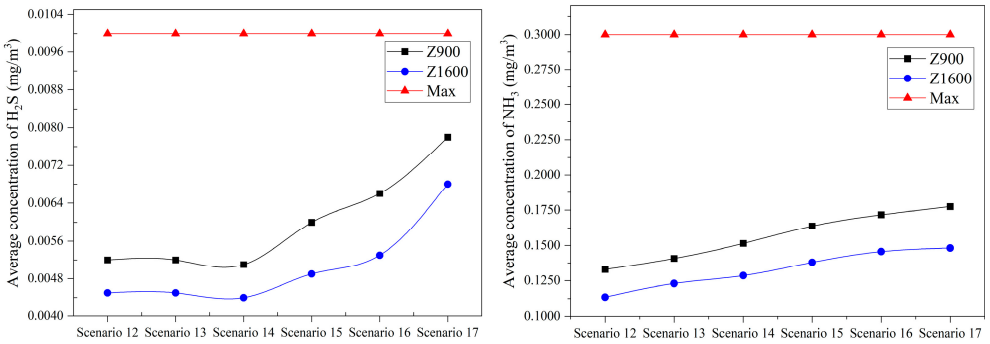

(**a**) (**b**)

Figure 11. Variation trend in the ACIPs for different exhaust vent heights. (**a**) Average concentration of H_2S; (**b**) Average concentration of NH_3.

Figure 11 shows the average concentration of indoor pollution as a function of the exhaust vent height. The ceiling limit value is the maximum ACIPs specified in the Hygienic Standard for Communal Toilets in Cities.

4. Discussion

In the traditional architectural design field, the experience of architectural designers is often vague and difficult to grasp, so this experience is difficult to use as the basis for accurate judgments. BIM contains the geometric information and attributes information of buildings. The combination of BIM, BEM, and CFD modeling can reduce data inconsistencies and errors.

4.1. Sensitivity Analysis

Studies have continuously been conducted to improve the IQA in public toilets. According to Section 3.1, the ACIPs are negatively correlated with the frequency of air exchanges, and the energy consumption gradually increases with the increase in the frequency of air exchanges. Therefore, according to the calculation results in Section 3.5, Table 12

shows the frequency of the air exchange boundary conditions for the all-air air conditioning system that we used to study the effect of different air exchange frequencies on the ACIPs.

Table 12. Boundary conditions of side exhaust air for different frequencies of air exchanges.

Scenario	Exhaust Outlet Height (mm)	Frequency of Air Exchanges (h^{-1})	Frequency of Air Exchanges (h^{-1})	Supply-Air Velocity (m/s)	Air-Outlet Velocity (m/s)
18	100/400/700	14	3893.4	3.13	3.03
19		13	3615.3		
20		12	3337.2		
21		11	3059.1		
22		10	2781.0		
23		9	2502.9		
24		8	2224.8		
25		7	1946.7		
26		6	1668.6		
27		5	1390.5		

Figure 12 shows the negative correlation of energy consumption with the ACIPs with different air exchange frequencies in the all-air air conditioning system and the positive correlation between the building energy consumption with the frequency of air exchanges. The intersection of the ACIPs and building energy consumption occurs in Scenario 22 (i.e., the frequency of air exchange is 10 h^{-1}). According to the calculation results, when the frequency of air exchange is between 11 and 15 times per hour, the ACIPs meets the requirements of the Hygienic Standard for Communal Toilets in Cities.

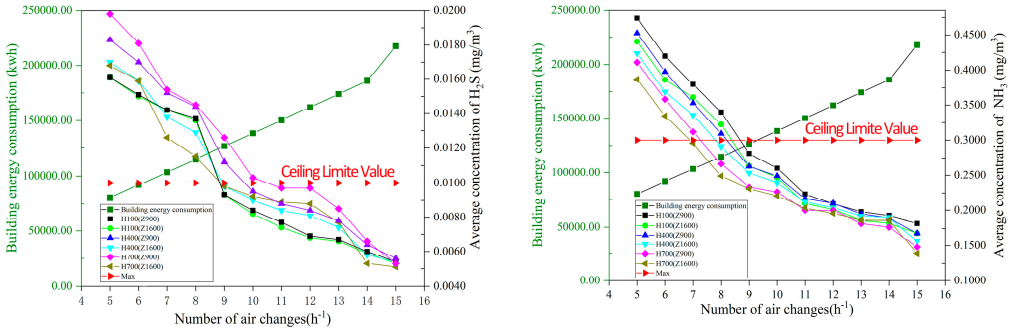

(**a**) (**b**)

Figure 12. Relationship between energy consumption and the ACIPs. (**a**) Relationship between energy consumption and the average concentration of H_2S; (**b**) Relationship between energy consumption and the average concentration of NH_3;

In the design phase of public toilets, the use of digital twins can improve the accuracy of the design and verify the impact of the diffusion of indoor pollutants in real environments. Digital twin evaluation can be combined with the building information models, CFD simulations and building energy consumption simulations to evaluate the current state, diagnose problems in different design scenarios, produce analyses results, simulate various possibilities, and provide more comprehensive decision support.

4.2. Evaluation Analysis

Our aim was to study the effects of different air exchange frequencies and exhaust vents heights on the diffusion of pollutants in public toilets. By simulating variations in parameters such as ventilation methods, air exchange frequency, and exhaust vent height and comparing ventilation efficiency and concentrations of indoor pollutants, a reasonable working plan could be constructed to guide the actual project.

The variation trend in the ventilation efficiency with different exhaust vent heights and air exchange frequencies is shown in Figure 13 (H100 represents that the height of the exhaust outlet is 100 mm). With the increase in ventilation frequency, the ventilation efficiency gradually increased, but the maximum increase in H_2S is 0.13, and the ventilation efficiency of ammonia gas increases by 2.94%. With the increase in the frequency of air exchanges, the ventilation efficiency gradually increases, but the maximum increase in H_2S is 0.13% and the maximum increase in NH3 ventilation efficiency is 2.94%. With the increase in the height of the exhaust vent, the ventilation efficiency gradually decreases, and the maximum reduction in H_2S and NH_3 ventilation efficiency is 0.42% and 5.25%, respectively. Therefore, the closer the exhaust vent to the pollution source and the higher frequency of air exchange, the more conducive it is to the removal of pollutants.

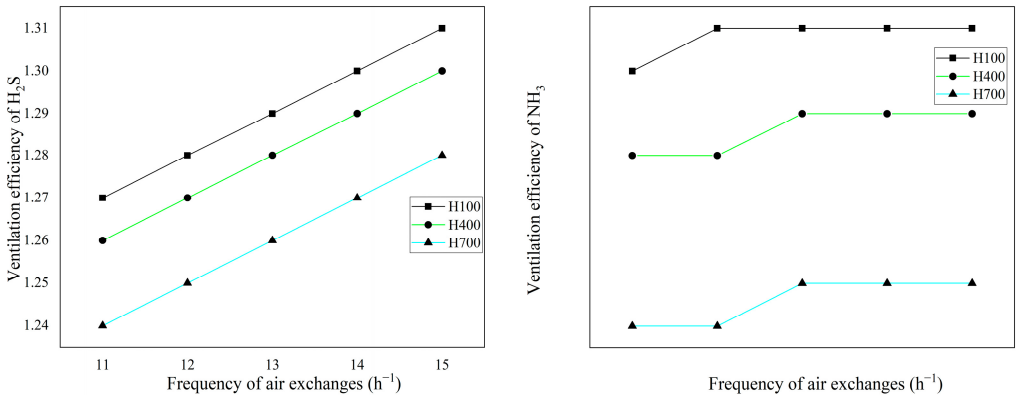

Figure 13. The relationship between ventilation efficiency and the frequency of air exchange. (**a**) Ventilation efficiency of H_2S; (**b**) Ventilation efficiency of NH_3.

Figure 14 shows the effect of different exhaust vent heights as a function of the frequency of air exchange. With the increase in the frequency of air exchange, the AOA gradually decreases, and the maximum reduction produced with an air exchange rate of 15 h^{-1} is 3.79% (Z700) compared to 11 h^{-1}. The height of the exhaust vent is 400 mm, which has advantages over other heights, which reduces the age of the air by 0.49% (Z100) and 0.84% (Z700). Therefore, the higher the height of the exhaust vent (i.e., 400 mm), the better the IAQ. Figure 15 shows the values of indoor comfort indicators *PMV* and PDD for different frequencies of air exchange. The results show that *PMV* and PDD tend to be stable with an increase in the frequency of air exchange.

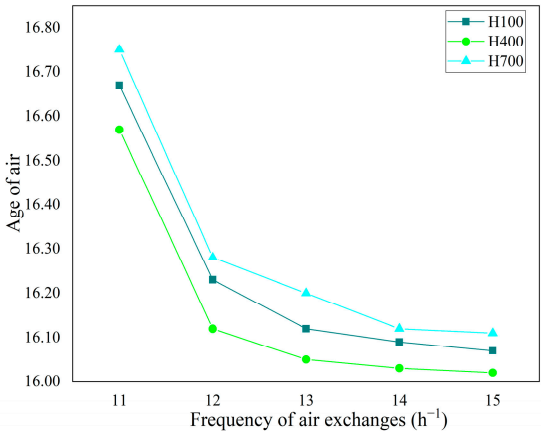

Figure 14. Age of air.

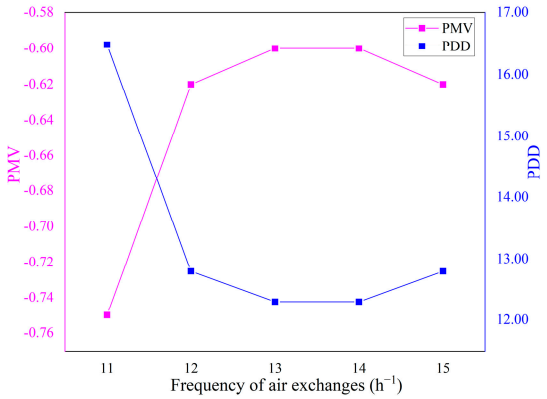

Figure 15. Comfort evaluation.

To optimize the airflow of public toilets and improve their IAQ, we adopted linear normalization ($X_{new} = (X_i - X_{min})/(X_{max} - X_{min})$ to analyze the combined effect of the ACIPs (concentrations of NH_3 (CNH) and H_2S (CHS)), ventilation efficiency (ventilation efficiency of NH_3 (VENH) and H_2S (VEHS)), the AOA, thermal comfort (*PMV* and PDD), and building energy consumption (BEC).

The purpose of indoor ventilation is to ensure human safety, comfort, health, and IQA. Figure 16 shows the normalized impact value for different vent heights and the air exchange frequencies. The normalized comprehensive influence value is the smallest when the height of the exhaust vent is 400 mm and the frequency of air exchanges is 12 h^{-1} (Figure 17). Therefore, the best form of air conditioning, in this case, is an all-air air conditioning system, with a frequency of air exchange of 12 h^{-1}, a supply-air velocity of 3.13m/s, and an exhaust vent height of 400 mm, and an exhaust vent velocity of 3.03m/s.

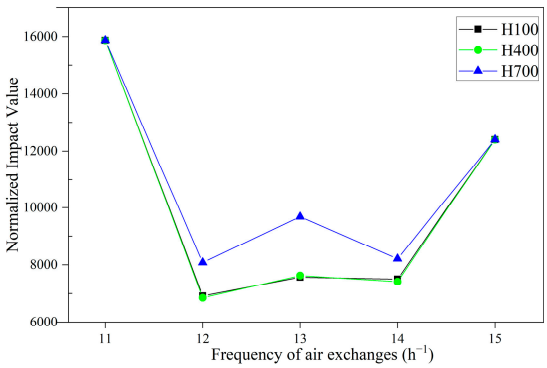

Figure 16. Normalized analysis.

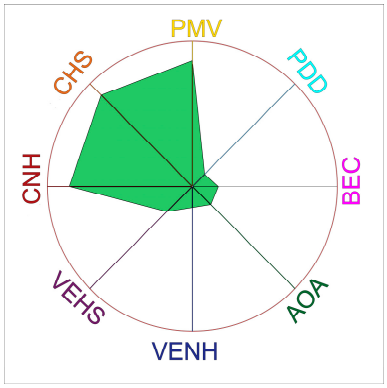

Figure 17. Normalized analysis comprehensive impact value.

5. Conclusions and Future Work

We proposed an integrated BIM, CFD, and BEM method for indoor pollutant optimization. We proposed solutions to ensure low concentrations of indoor pollutants in public toilets, optimal thermal comfort, low energy consumption, and low carbon emissions. We used Fluent and Design Builder software to simulate the indoor environment and energy consumption of public toilets, and compared and analyzed the effects of two common ventilation and air conditioning systems (primary air fan–coil system and all-air air conditioning system) on indoor pollutant diffusion, and we drew the following conclusions:

The computational results showed a series of simulations that were performed using a BIM-based digital twin. These simulation results were used to determine the airflow organization and changes in the concentrations of indoor pollutants in a public toilet through the digital twin model to recommend the design of the ventilation system. BIM-based digital twins can be used to evaluate the distribution of the ACIPs in public toilets, and obtain a large amount of valuable data regarding the air conditioning system, the frequency of air exchange, and the exhaust vent height. According to the ACIPs, ventilation efficiency, the age of the air, *PMV*, and PDD, the simulation results provide a basis for designers to make decisions, thereby helping designers to select the most effective ventilation design to improve the environment and safety of public toilets.

BIM-based digital twins can also be used for a range of other building design improvements and decisions because BIM can provide rich geometric, attribute, and relationship information. By establishing a BIM of different indoor ventilation scenarios and simulating public toilets with their digital twin models, a reference can be provided for the ventilation design of public toilets. These simulations can be extended to evaluate other types of building ventilation designs. For example, changing the population density and ventilation method will impact the distribution of aerosols in the room, so a reasonable population density and ventilation control method can be devised to reduce the current risk of COVID-19 infection.

The all-air air conditioning system and air discharge using an exhaust vent height of 400 mm can considerably reduce the ACIPs in public toilets and ensure the IAQ. A 12 h^{-1} air ventilation frequency can reduce energy consumption by 25.55% compared to 15 h^{-1}, and reduce carbon emissions by 39,130.54 kg CO_2.

In future work, this study will be extended to building cost and construction simulations. Based on these data, the cost of the building can be considered to predict the cost information for different scenarios. These data must be obtained to ensure the smooth implementation of public toilets. These additional simulation data will be provided by professional companies, which will allow for more realistic simulations. The future study will focus on a collaboration with the IOTWINS (Distributed Digital Twins for industrial SMEs: a big-data platform), which provides cloud-based tools and services for (but not limited to) the hybrid digital twins. Adopting cloud-based services can improve the quality and definition of digital twins, reducing computation time and results sharing. In the future, machine learning to speed-up computation can be used, and a GPU can be used to run simulation tools to improve efficiency.

Author Contributions: Conceptualization, L.Z., H.Z., Q.W., and X.S.; data curation, B.S., W.L. and K.Q.; formal analysis, H.Z., Q.W.; funding acquisition, L.Z.; methodology, X.S., H.Z. and Q.W.; resources, L.Z., H.Z., Q.W. and B.S.; software, B.S. and K.Q.; supervision, L.Z.; validation, L.Z.; visualization, L.Z. and B.S.; writing–original draft, H.Z., Q.W. and L.Z.; writing–review & editing, L.Z. and W.L. All authors have read and agreed to the published version of the manuscript.

Funding: This study was funded by the Research on the Technologies of Passenger Stations in Beijing–Tianjin–Hebei region (Grant no. P2018G049) and the Key Laboratory of Urban and Architectural Heritage Conservation, Ministry of Education, Southeast University (Grant no. KLUAHC1905).

Institutional Review Board Statement: Not applicable.

Informed Consent Statement: Not applicable.

Data Availability Statement: Not applicable.

Conflicts of Interest: The authors declare no conflict of interest.

References

1. Wang, C.H. Numerical Simulation of Pollutant Diffusion and Ventilation Control in Public Building Toilets. Master's Thesis, Xi'an University of Architecture and Technology, Xi'an, China, 2020. (In Chinese).
2. Norling, M.; Stenzelius, K.; Ekman, N.; Wennick, A. High School Students' Experiences in School Toilets or Restrooms. *J. Sch. Nurs.* **2016**, *32*, 164–171. [CrossRef]
3. Verani, M.; Bigazzi, R.; Carducci, A. Viral contamination of aerosol and surfaces through toilet use in health care and other settings. *Am. J. Infect. Control* **2014**, *42*, 758–762. [CrossRef]
4. Zhang, Z.; Zeng, L.; Shi, H.; Liu, H.; Yin, W.; Gao, J.; Wang, L.; Zhang, Y.; Zhou, X. CFD studies on the spread of ammonia and hydrogen sulfide pollutants in a public toilet under personalized ventilation. *J. Build. Eng.* **2022**, *46*, 103728. [CrossRef]
5. The State Bureau of Quality and Technical Supervision; Ministry of Health of the People's Republic of China. *Hygienic Standard for Communal toilet in City (GB/T 17217-1998)*; Ministry of Health of the People's Republic of China: Beijing, China, 1998.
6. Ministry of Housing and Urban Rural Development of the People's Republic of China. *Standard for Design of Urban Public Toilets (CJJ 14-2016)*; Ministry of Health of the People's Republic of China: Beijing, China, 2016.
7. Anghel, L.; Popovici, C.G.; Statescu, C.; Sascau, R.; Verdes, M.; Ciocan, V.; Serban, I.L.; Maranduca, M.A.; Hudisteanu, S.V.; Turcanu, F.E. Impact of HVAC-Systems on the Dispersion of Infectious Aerosols in a Cardiac Intensive Care Unit. *Int. J. Environ. Res. Public Health* **2020**, *17*, 6582. [CrossRef]
8. Sun, S.; Han, J. Open defecation and squat toilets, an overlooked risk of fecal transmission of COVID-19 and other pathogens in developing communities. *Environ. Chem. Lett.* **2020**, *19*, 787–795. [CrossRef]
9. Lee, M.; Park, G.; Jang, H.; Kim, C. Development of Building CFD Model Design Process Based on BIM. *Appl. Sci.* **2021**, *11*, 1252. [CrossRef]
10. Gu, D.; Zheng, Z.; Zhao, P.; Xie, L.; Xu, Z.; Lu, X. High-Efficiency Simulation Framework to Analyze the Impact of Exhaust Air from COVID-19 Temporary Hospitals and its Typical Applications. *Appl. Sci.* **2020**, *10*, 3949. [CrossRef]
11. Wan, M.P.; Chao, C.Y. Transport characteristics of expiratory droplets and droplet nuclei in indoor environments with different ventilation airflow patterns. *J. Biomech. Eng.* **2007**, *129*, 341–353. [CrossRef]
12. Ascione, F.; De Masi, R.F.; Mastellone, M.; Vanoli, G.P. The design of safe classrooms of educational buildings for facing contagions and transmission of diseases: A novel approach combining audits, calibrated energy models, building performance (BPS) and computational fluid dynamic (CFD) simulations. *Energy Build.* **2021**, *230*, 110533. [CrossRef]
13. Bhattacharyya, S.; Dey, K.; Paul, A.R.; Biswas, R. A novel CFD analysis to minimize the spread of COVID-19 virus in hospital isolation room. *Chaos Solitons Fractals* **2020**, *139*, 110294. [CrossRef]
14. Li, Y.; Leung, G.M.; Tang, J.W.; Yang, X.; Chao, C.Y.; Lin, J.Z.; Lu, J.W.; Nielsen, P.V.; Niu, J.; Qian, H.; et al. Role of ventilation in airborne transmission of infectious agents in the built environment—A multidisciplinary systematic review. *Indoor Air.* **2007**, *17*, 2–18. [CrossRef]
15. Peng, Y.; Zhang, M.; Yu, F.; Xu, J.; Gao, S.; Rodrigues, H. Digital Twin Hospital Buildings: An Exemplary Case Study through Continuous Lifecycle Integration. *Adv. Civ. Eng.* **2020**, *2020*, 1–13. [CrossRef]
16. Ao, Y.G.; Wang, L.; Jia, X.; Gu, C. Numerical Simulation of Pollutant Diffusion Law in Bathroom and Optimization of the Locations and Ways of Exhaust Outlet and Makeup Air. *J. Shenyang Jianzhu Univ.* **2011**, *4*, 720–725. (In Chinese)
17. Lu, Q.; Chen, L.; Li, S.; Pitt, M. Semi-automatic geometric digital twinning for existing buildings based on images and CAD drawings. *Autom. Constr.* **2020**, *115*, 103183. [CrossRef]
18. Khajavi, S.H.; Motlagh, N.H.; Jaribion, A.; Werner, L.C.; Holmstrom, J. Digital Twin: Vision, Benefits, Boundaries, and Creation for Buildings. *IEEE Access.* **2019**, *7*, 147406–147419. [CrossRef]
19. Zhao, L.; Zhang, H.; Wang, Q.; Wang, H.; Dede, T. Digital-Twin-Based Evaluation of Nearly Zero-Energy Building for Existing Buildings Based on Scan-to-BIM. *Adv. Civ. Eng.* **2021**, *1–11*, 6638897. [CrossRef]
20. Delavar, M.; Bitsuamlak, G.T.; Dickinson, J.K.; Costa, L.M.F. Automated BIM-based process for wind engineering design collaboration. *Build. Simul.* **2019**, *13*, 457–474. [CrossRef]
21. Guo, M.Y.; Xu, P.; Xiao, T.; He, R.K.; Dai, M.K. Comparison of existing HVAC operation guidelines for COVID-19 pandemics. *Heat. Vent. Air Cond.* **2020**, *11*, 13–20. (In Chinese)
22. Ministry of Housing and Urban Rural Development of the People's Republic of China. *Design Code for Heating Ventilation and air Conditioning of Civil Buildings (GB50376-2012)*; Ministry of Housing and Urban-Rural Development of the People's Republic of China: Beijing, China, 2012.
23. Wen, Y.; Leng, J.; Yu, F.; Yu, C.W. Integrated design for underground space environment control of subway stations with atriums using piston ventilation. *Indoor Built Environ.* **2020**, *29*, 1300–1315. [CrossRef]
24. Ministry of Housing and Urban Rural Development of the People's Republic of China. *National Technical Measures for Design of Civil Construction: Heating, Ventilation and Air Conditioning-2017*; Ministry of Housing and Urban Rural Development of the People's Republic of China: Beijing, China, 2017.

25. Ding, Z.; Qian, H.; Xu, B.; Huang, Y.; Miao, T.; Yen, H.L.; Xiao, S.; Cui, L.; Wu, X.; Shao, W.; et al. Toilets dominate environmental detection of severe acute respiratory syndrome coronavirus 2 in a hospital. *Sci Total Environ.* **2021**, *753*, 141710. [CrossRef]
26. Cheng, V.C.; Wong, S.C.; Chan, V.W.; So, S.Y.; Chen, J.H.; Yip, C.C.; Chan, K.H.; Chu, H.; Chung, T.W.; Sridhar, S.; et al. Air and environmental sampling for SARS-CoV-2 around hospitalized patients with coronavirus disease 2019 (COVID-19). *Infect Control Hosp. Epidemiol.* **2020**, *41*, 1258–1265. [CrossRef] [PubMed]
27. Lou, M.; Liu, S.; Gu, C.; Hu, H.; Tang, Z.; Zhang, Y.; Xu, C.; Li, F. The bioaerosols emitted from toilet and wastewater treatment plant: A literature review. *Environ. Sci. Pollut. Res. Int.* **2021**, *28*, 2509–2521. [CrossRef] [PubMed]
28. Johnson, D.L.; Mead, K.R.; Lynch, R.A.; Hirst, D.V. Lifting the lid on toilet plume aerosol: A literature review with suggestions for future research. *Am. J. Infect. Control.* **2013**, *41*, 254–258. [CrossRef] [PubMed]
29. Zhao, Q.; Lian, Z.; Lai, D. Thermal comfort models and their developments: A review. *Energy Built Environ.* **2021**, *2*, 21–33. [CrossRef]
30. Zahid, H.; Elmansoury, O.; Yaagoubi, R. Dynamic Predicted Mean Vote: An IoT-BIM integrated approach for indoor thermal comfort optimization. *Autom. Constr.* **2021**, *129*, 103805. [CrossRef]
31. Lin, P.-H.; Chang, C.-C.; Lin, Y.-H.; Lin, W.-L. Green BIM Assessment Applying for Energy Consumption and Comfort in the Traditional Public Market: A Case Study. *Sustainability* **2019**, *11*, 4636. [CrossRef]
32. General Administration of Quality Supervision, Inspection and Quarantine of the People's Republic of China. *Ergonomics of the Thermal Environment—Analytical Determination and Interpretation of Thermal Comfort Using Calculation of the PMV and PPD Indices and Local Thermal Comfort Criteria (GB/T 18049-2017 ISO 7730:2005)*; Standardization Administration of the People's Republic of China: Beijing, China, 2017.